

Single molecule imaging reveals cFos is capable of binding to and diffusing on DNA tightropes independently of cJun

James T. Leech¹, Nicola A. Don², Jody M. Mason³ and Neil M. Kad¹

¹School of Biological Sciences, University of Kent, Canterbury, CT2 7NH, UK. ²Department of Biological Sciences, University of Essex, Colchester, CO3 4SQ, ³Department of Biology & Biochemistry, University of Bath, Bath, BA2 7AY, UK.

Please address correspondence to JMM (j.mason@bath.ac.uk) or NMK (n.kad@kent.ac.uk)

Key words: Quantum dots, DNA tightropes, Fluorescence, transcription factors, AP-1, bZIP

Abstract

AP-1 proteins are members of the basic leucine zipper (bZIP) protein family of dimeric transcription factors, responsible for controlling many integral cellular processes. These proteins form dimers with each other, and their aberrant expression can lead to a number of cancer types. The oncogenic transcription factor AP-1 binds its target TRE site (5'TCA[G/C]TGA), however the physical mechanism of how this is achieved is not understood. Such an understanding is essential to know how these proteins function, and could offer the potential to uncover new drug targets. The archetypal AP-1 complex is formed by cFos and cJun, which heterodimerise via their bZIP domains. Here, we set out to investigate how these proteins interact with DNA using a real-time single molecule fluorescence imaging approach. Using DNA tightropes as a substrate, we determine that the AP-1 bZIP dimers cJun:cFos and cJun:cJun rapidly scan DNA using a 1D diffusional search with an average diffusion constant of $0.14 \mu\text{m}^2\text{s}^{-1}$ and $0.26 \mu\text{m}^2\text{s}^{-1}$ respectively. Remarkably, we also found that cFos was able to bind to and diffuse on DNA ($0.29 \mu\text{m}^2\text{s}^{-1}$) both as a monomer and homodimer. Periods of diffusion were punctuated by pauses, suggesting a mechanism for how AP-1 may rapidly find its target sites on DNA. Taken together the results we have obtained indicate a considerably more complex and graded interaction between cFos, cJun and DNA than has been reported previously.

Introduction

Activator Protein 1 (AP-1) is a group of dimeric transcription factors composed of members of the Jun, Fos and ATF protein families (1). Individual AP-1 proteins possess leucine zipper regions for dimerization and basic regions for DNA binding, a motif common to all bZIP proteins (2,3). bZIP proteins in general are capable of forming homo- and hetero- dimers, which increases the diversity of function from a limited number of proteins. Such functions identified for AP-1 complexes include cell proliferation, differentiation, repair, and response to stress (1,4-7). These complexes are involved in immediate-early gene pathways (8), allowing rapid modulation of transcriptional profiles in response to stressors such as viral infection (9). Furthermore, AP-1 complexes have been strongly implicated in the development of cancer (10-12); and aberrant expression or activity of AP-1 proteins leads to uncontrolled proliferation and angiogenesis in tumours (13). Therefore, understanding how AP-1 binds DNA has significant value for the development of novel cancer therapeutics (14,15).

The archetypal and most well-studied AP-1 complex is the cJun:cFos heterodimer, which binds and activates transcription at the 12-O-tetradecanoylphorbol-13-acetate (TPA) response element (TRE), with a 7 bp consensus sequence TGA[G/C]TCA (2,16). cJun:cFos is also capable of binding the 8 bp consensus sequence TGACGTCA from the cyclic-AMP response element (CRE), with a similar reported affinity to TRE (17,18). These AP-1 binding sites have been largely deselected from the mammalian genome except in specific promoters, which often contain more than one binding site (19). In the absence of cFos, cJun has been shown to homodimerize and bind TRE/CRE sites with a lower affinity (2,20), but nonetheless activate transcription (21). Several previous studies have suggested that cFos is incapable of homodimerization and binding DNA, due to poor interaction dynamics within the leucine zipper (2,14). While isolated cFos leucine zippers have been shown to display a weak unstable interaction (22), cFos has been defined as a DNA-binding protein and transcription factor only in the presence of cJun (23), which brings significant additional hydrophobicity to the leucine zipper core. Despite this, a recent *in vivo* study has revealed that cFos may be able to form homodimers (24).

In this study we address the diversity of complexes formed between cJun and cFos using direct single molecule imaging. By differentially tagging AP-1 proteins with quantum dots (Qdots) and visualizing their interaction on DNA tightropes (single DNA molecules suspended between 5-micron high platforms), we are able to determine which complexes form and their relative prevalence. As expected, cJun was observed to form homodimers and to heterodimerise with cFos. However, cFos was unexpectedly found to bind DNA tightropes in the absence of cJun, both as monomers and dimers. This provides confirmatory evidence that cFos can bind DNA independently of AP-1 partners, indicating the existence of a new and potentially important member of the AP-1 transcription factor family. In addition, our approaches provide quantitative characterisation of the target search mechanisms employed by each protein combination (25,26). These physical properties affect their search capabilities, and we also suggest a mechanism for the differential affinities for target and non-target sequences.

Materials and Methods

Synthesis of cFos and cJun

Protein sequences 137-193 and 252-308 from human cFos (UniProt code - P01100) and cJun (UniProt code - A0A510GAI3) respectively were synthesized with a C-terminal biotin. Peptides were

synthesized by Protein Peptide Research Ltd, Eastleigh, U.K. Correct masses were verified by electrospray mass spectrometry. cFos and cJun refer to the bZIP domains only and do not include transactivation or other domains.

Single Molecule DNA Tightrope Assay

Unmodified bacteriophage Lambda DNA (NEB) was used in all assays. Lambda DNA is 48,502 bp and contains 8 TRE and 1 CRE consensus sites along its length.

Flow cells and DNA tightropes were constructed as described previously (26). All experiments were performed in a buffer composed of 150 mM KCl, 50 mM Tris and 10 mM MgCl₂ (pH 7.5), termed HSABC.

Protein Conjugation

To enable fluorescence imaging, biotinylated proteins were conjugated with streptavidin-tagged Qdots, specifically Qdot 655 and Qdot 605 (Thermo Fisher). Proteins were incubated at a concentration of 100 nM in HSABC with 200 nM Qdots for a minimum of 20 minutes on ice. Proteins were then diluted to 2 nM (4 nM Qdots) and applied to DNA tightropes. In homodimer experiments, Qdots were premixed and then applied to proteins to allow an equal chance of the protein conjugating with either colour Qdot. In heterodimer experiments, cJun and cFos proteins were conjugated separately, then mixed together at a concentration of 2 nM each. The mixture was heated to 42°C for 10 minutes to permit monomer dissociation, then cooled to room temperature for at least 10 minutes to enable reselection of dimeric partners. This was based on previously determined dimer melting temperatures (23).

Microscopy

Visualisation of DNA tightropes was performed using a custom-built oblique angle fluorescence microscope at room temperature (20°C) as described previously (26). Fluorescence excitation was achieved using an Oxxius 488nm laser at 5 mW, guided into the microscope at a sub-critical angle to generate a far-field. Images were captured using a Hamamatsu ORCA-Flash4.0 V2 sCMOS camera at 10 Hz after colour splitting through an Optosplit III (Cairn Research Ltd). The three colour channels were 500-565 nm, 565-620 nm and 620-700 nm and the pixel resolution was measured as 63.2 nm.

Image analysis

60 second videos were collected at a frame rate of 10 fps using 1x1 binning. A custom ImageJ macro was used to fit kymographs of individual Qdots to a 1D Gaussian distribution (available from kadlab.mechanicsanddynamics.com). The resulting data were used to calculate the mean squared displacement (MSD, see (27)), which were subsequently fitted (Microsoft Excel's solver) to obtain 1D diffusion constants (D) and diffusive exponent values (α). To do this, 10-20% of the data was used to create linear (time vs MSD) and logarithmic (log-time vs log-MSD) graphs. A linear trendline was applied to the logarithmic graph and the data was only used if the R^2 was above 0.9. For these datasets a linear trendline was then applied to the linear graph, if the trendline had an R^2 above 0.9, the signal was classified as randomly diffusing, whereas if the R^2 was below 0.9, the kymograph was classified as pausing. The 1D diffusion constant represents the diffusivity of a molecule on DNA; a higher value indicates more rapid diffusion. The diffusive exponent value reveals the diffusive behaviour of a molecule, a value of 1 represents a random walk, below 1 can be caused by pausing, and above 1 represents directed motion (28). All errors are reported as standard error of the mean (SEM), and were calculated based on the number of flow cells rather than the number of molecules tracked (n =

50). To achieve 50 analysable tracks several hundred molecules needed to be imaged and analysed, since only high quality kymographs could be used.

Static molecules were classified as follows. A set of 10 kymographs were selected which showed no significant movement along their tracks, i.e. did not deviate more than two pixels from their start point in 60 seconds. Diffusion constants for these kymographs were calculated and averaged, yielding a threshold of $6.97 \times 10^{-5} \mu\text{m}^2\text{s}^{-1}$. Molecules with diffusion constants below this threshold were classified as static and omitted from diffusion dynamics calculations.

Qdot blinking

The Gaussian kymograph fitting algorithm used above would also attempt to fit frames with only the background fluorescent signal, i.e. during Qdot blinks. When doing so, fits with visible blinks were found to be consistently poor with the quality parameter $R^2 < 0.7$, compared with > 0.9 for accurate fitting. Using this criterion, we filtered the fits to determine number and duration of blinks. The average length of a blink in these experiments was 1.48 ± 0.089 frames or 0.148 seconds.

Results

Quantification of AP-1 behaviour on DNA tightropes

To study the DNA binding and search mechanisms of AP-1 peptides we conjugated the bZIP regions of cJun and cFos with Qdots to provide bright and photostable fluorescence emission. These proteins were then incubated with DNA tightropes; single DNA molecules suspended between surface-immobilised beads, and imaged using fluorescence microscopy (Figure 1A; (25,26)). We studied both single colour and dual colour labelled AP-1 proteins in these experiments, since it is well established that they form dimers (2,29). Figure 1B shows clear binding of cJun to DNA at 2 nM, and its motion is revealed as a kymograph in Figure 1C. Fitting MSDs obtained from the kymographs (see methods) provided values for the average diffusion dynamics. For cJun the diffusion constant and diffusive exponent were $7.5 \pm 3.9 \times 10^{-3} \mu\text{m}^2\text{s}^{-1}$ and 0.8 ± 0.09 respectively. This value includes the presence of Qdots, which increase the hydrodynamic drag of a diffusing molecule. We corrected for the presence of Qdots by taking into consideration the friction of the protein moving on the DNA (termed energy barrier here). Details of this calculation are provided in the supplementary information and (27,30). We calculated an average energy barrier of 1.1 kT , which gives a diffusion constant for cJun alone of $0.26 \pm 0.13 \mu\text{m}^2\text{s}^{-1}$.

Unexpectedly, we were also able to detect the binding of cFos to DNA. The average diffusion constant for cFos was similar to cJun at $8.4 \pm 4.1 \times 10^{-3} \mu\text{m}^2\text{s}^{-1}$ and the diffusive exponent was 0.69 ± 0.099 . Correcting for the Qdot as above for cJun, the diffusion constant for cFos was $0.29 \pm 0.14 \mu\text{m}^2\text{s}^{-1}$ with an energy barrier of 1.0 kT . The remarkable observation of cFos binding to DNA prompted us to investigate its stoichiometry of binding using dual colour labelling. Qdots (655 nm and 605 nm) were premixed prior to cFos conjugation to allow an equal chance of a protein binding either coloured Qdot. The expected proportion of dual colour signals for homodimer formation would be 50%, since 25% of the molecules would dimerise with Qdots of the same colour. Surprisingly only $15\% \pm 1.9$ of cFos molecules bound to DNA as dual coloured entities, suggesting that a sizeable proportion of observed cFos molecules were bound to DNA as monomers (Figure 2). To ensure that this was not an artefact of labelling we also studied the occurrence of dual colour signals for cJun. We found $47\% \pm 1.3$ were dual coloured consistent with 100% of the DNA-bound entities being dimers; additionally, this confirms that one Qdot binds per protein and does not interfere with dimerization.

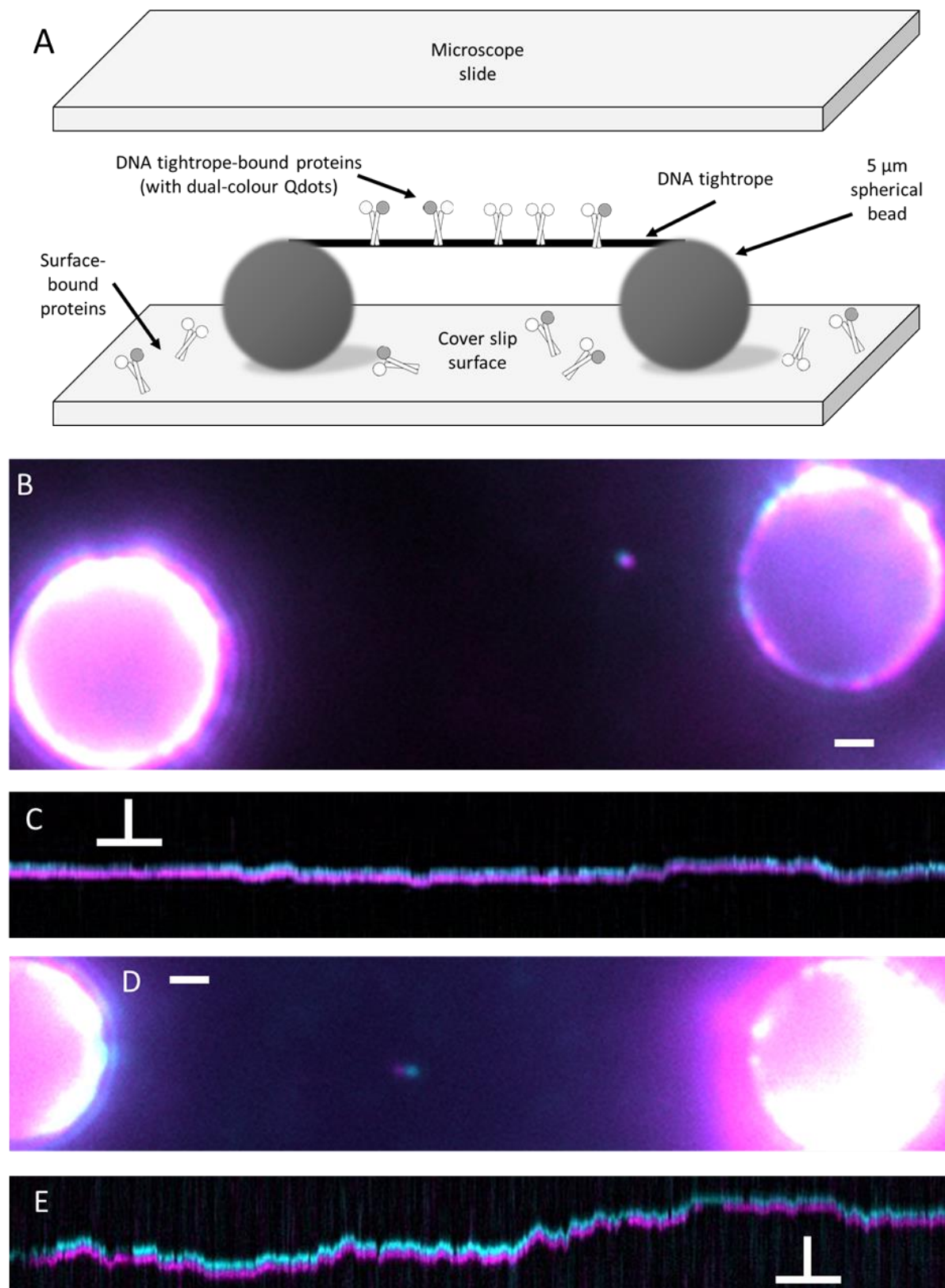


Figure 1: Imaging AP-1 interactions with DNA using tightropes. A – Diagrammatic representation of a DNA tightrope bound with AP-1 proteins and suspended between two surface adhered glass beads. B – Dual colour image of a cJun:cJun homodimer showing colocalization of Qdots. C – A kymographic representation of cJun:cJun homodimer position through time, showing clear diffusion on the tightrope. D – Dual colour image of a cFos:cFos homodimer bound to a DNA tightrope. E – Both Qdots are seen

to diffuse on the DNA confirming the existence of a cFos:cFos homodimer. Scale bars in images = 1 μ m. Scale bars in kymographs = 5 seconds (horizontal) vs 1 μ m (vertical).

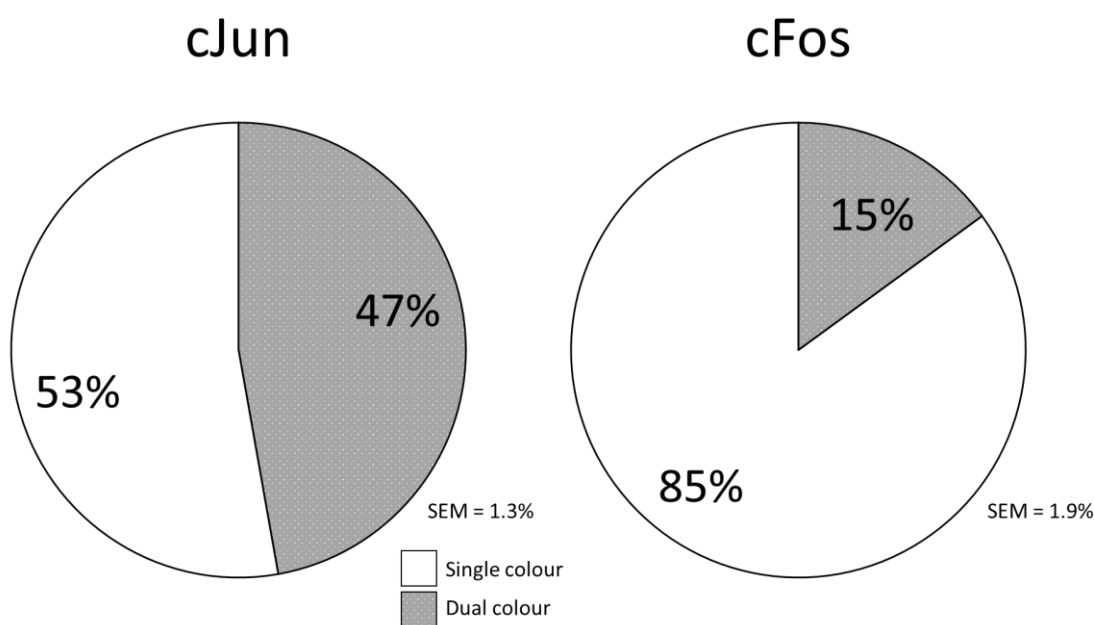


Figure 2: Pie charts indicating the proportion of dual and single colour signals observed for cJun and cFos. Proteins were conjugated with mixed Qdots 655 and 605. A population of 100% homodimers would be expected to exhibit a proportion of 50% dual colour signals. A proportion of less than 50% dual colour signals indicates the presence of monomers (n = 638 cJun, 597 cFos, 3 flow cells for each). Therefore, cJun forms nearly 100% dimers whereas cFos is predominantly monomeric.

Using Qdot Blinking to Determine Oligomeric State

Dual colour imaging suggests that cJun binds predominantly as a dimer, but for cFos fewer dimers were seen. Since 15% of molecules were dual coloured and therefore dimers, this would mean that 15% of the single coloured molecules were also dimers. Therefore, 70% of the total DNA-bound molecules were cFos in the monomeric form. Due to the photophysical properties of Qdots that result in non-uniform fluorescence emission (31), it is not possible to determine the proportion of single coloured dimerised complexes using fluorescence intensity. Instead, analysis of Qdot blinking was used as an indication of the oligomeric state. The chance of a molecule dropping to a completely dark state will be reduced if there are two Qdots present since the probability is the square of that from a single Qdot, resulting in 'fluorescence redundancy'. The number of blink events were calculated from 50 kymographs (using Qdot 655 conjugates only) and displayed as a histogram (Figure 3). 58% of cJun kymographs exhibited between 0 and 4 blinks, compared to 20% for cFos. The histogram also displays a prominent peak between 9 and 12 blinks for cFos but not for cJun. This implies the presence of 2 populations: dimers with few blinks, and monomers with a greater number of blinks. The average numbers of blinks for cJun and cFos were 3.24 ± 3.48 and 10.58 ± 3.53 respectively, consistent with our inference of the presence of cFos monomers in the dual-colour experiments (Figure 2).

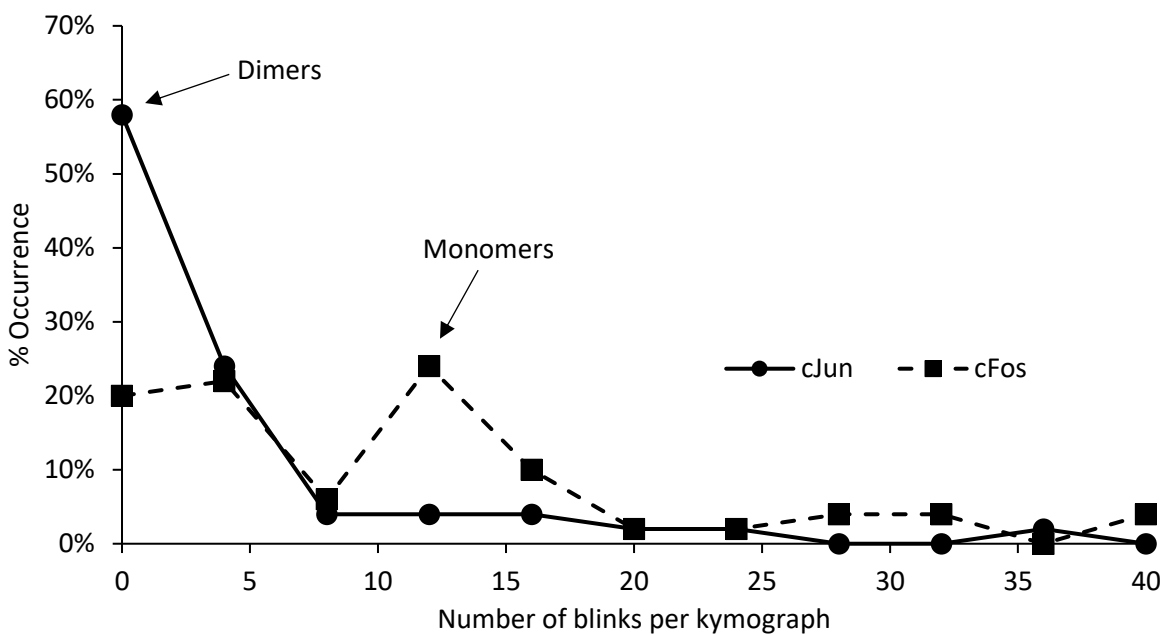


Figure 3: Analysis of quantum dot blinking to determine complex stoichiometry. The percentage occurrence of quantum dot blinks per kymograph for cJun (solid lines) and cFos (dashed lines) were plotted as a histogram. The dominance of zero for cJun indicates homodimer formation i.e. fluorescence redundancy of two Qdots. By contrast, cFos peaks at ~12 blinks per kymograph confirming the presence of monomers. All kymographs were identical in duration (60 s), n = 50 for each protein, 5 flow cells for cJun, 10 flow cells for cFos.

Observation of cJun:cFos Heterodimers on DNA

The leucine zipper of AP-1 mediates the ability of constituent proteins to dimerise, which in turn affects their function *in vivo*. We set out to image the formation of these heterodimers on DNA directly, by using dual colour imaging. Proteins were independently conjugated with different coloured Qdots, then mixed together at 2 nM before imaging on DNA tightropes (Figure 4A and B). The least prevalent signal (12%) detected was cJun:cFos, compared with cJun (57%) and cFos (31%) (Figure 4C). This was surprising because cJun:cFos has been previously shown to bind AP-1 sites at a greater affinity than cJun homodimers (2). Additionally, cJun:cFos has been shown to form a more thermodynamically-stable complex than cJun:cJun or cFos:cFos (14,23).

In addition to studying dimerization we were also able to measure the diffusional dynamics of this heterodimeric complex. From a total of 50 dual-colour cJun:cFos kymographs an average diffusion constant was measured as $4.0 \pm 2.6 \times 10^{-3} \mu\text{m}^2\text{s}^{-1}$. The heterodimer's average diffusive exponent value was 0.71 ± 0.15 , similar to cFos (0.69). As explained above, for the individual proteins we again corrected the diffusion constant for the presence of Qdots to $0.14 \pm 0.09 \mu\text{m}^2\text{s}^{-1}$, with a diffusional energy barrier of 1.8 kT.

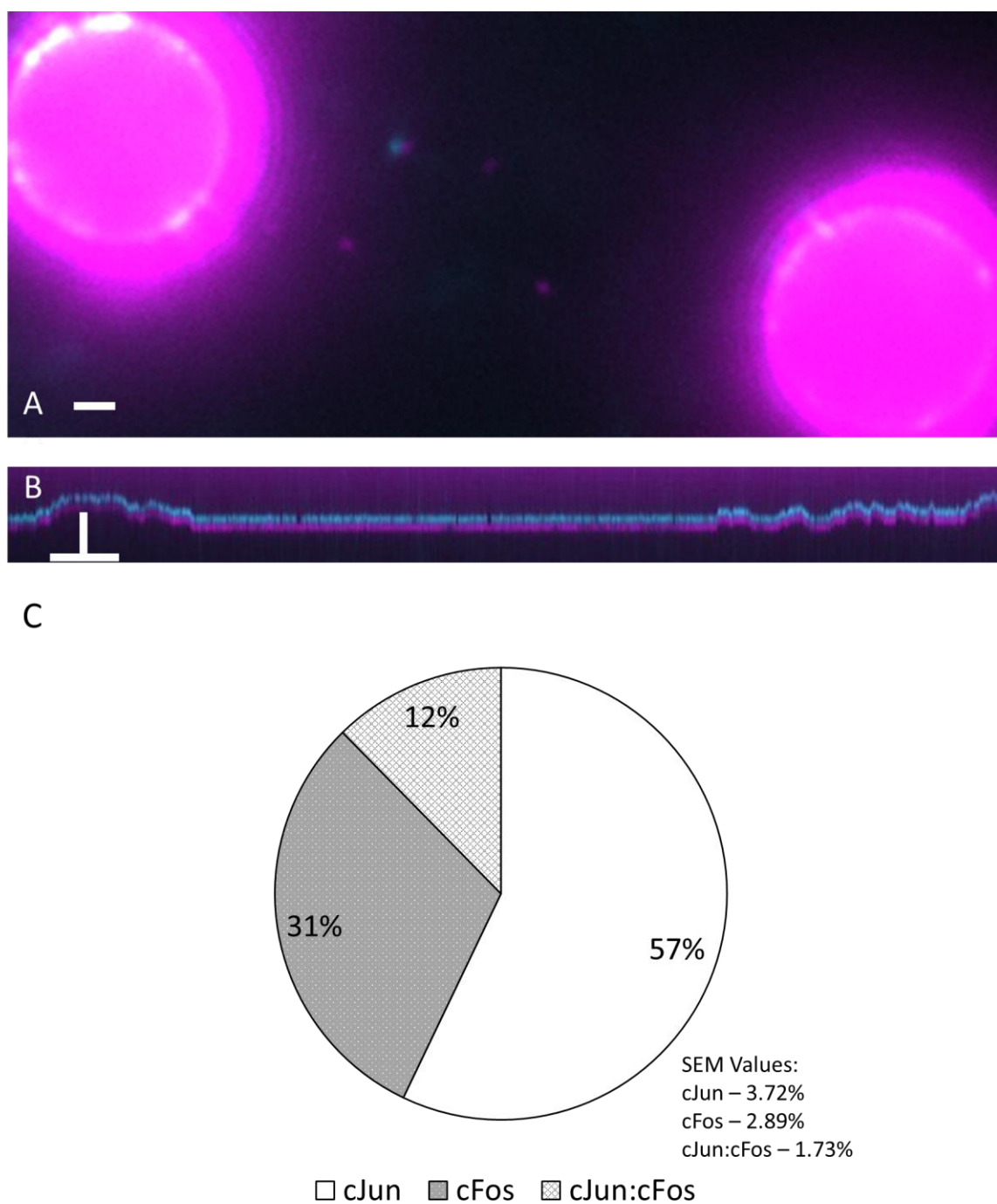


Figure 4: Dual colour imaging of cJun:cFos heterodimers. cJun was conjugated with Qdot 655 (magenta) while cFos was conjugated with Qdot 605 (cyan). The two conjugates were mixed at 2 nM and then heated to 42°C to dissociate homodimers, before cooling to room temperature and adding to lambda DNA tightropes. A – Merged channel image; scale bar represents 1 μm. Magenta-only signals indicate non-heterodimer cJun molecules. B – Merged channel kymograph shows diffusion of the heterodimeric complex; scale bars represent 5 seconds (horizontal) vs 1 μm (vertical). C – Proportions of proteins observed in dual colour experiments when cJun and cFos were mixed together and applied to DNA tightropes (total n = 429, 8 flow cells).

Discussion

The dimeric AP-1 transcription factor family control gene expression by binding specific promoter sequences. Using single molecule fluorescence imaging we have determined how homodimers and cJun:cFos heterodimers form on DNA. Surprisingly, we also detected the binding of cFos to DNA. Using a combination of dual colour imaging and blink analysis, we determined that cFos bound predominantly to DNA as monomers. This has not been previously reported and is in contrast to cJun, which bound exclusively as homodimers. In addition to determining binding stoichiometry, we have also determined how these complexes search for their target sites by imaging their positions through time.

cFos binds DNA as a monomer

The binding of cFos to DNA has not been definitively determined; the majority of preceding studies have used electrophoretic mobility shift assays to indicate that cFos does not interact alone with DNA (2,23). However, a recent study using FRET in live cells showed cFos binds DNA as a homodimer. Here, we were able to detect cFos interacting with DNA using direct single molecule imaging. Our studies show that cFos not only binds in homodimeric form to DNA as shown previously (24) but also as a monomer. Data from dual colour analysis suggests ~30% of cFos forms dimers. Using blink analysis (Figure 3), we show that in the first histogram bin 58% of kymographs show blinks, this compares with 20% for cFos. If we assume that the first bin corresponds to 100% dimers, as indicated for cJun in Figure 2, then cFos has ~1/3 the dimers of cJun, i.e. 33%; this estimate compares well with that obtained from the dual colour data (30%). The existence of monomeric DNA-bound cFos has not been reported previously, and would not be detectable using for example the FRET modality of the Szalóki study (24). Interestingly, our data suggest that the majority of cFos-DNA interactions occur from monomeric cFos (Figure 2). Perhaps one reason why this interaction between cFos and DNA has not been reported is that during EMSA studies the proteins are exposed to conditions of high shear within a gel. Transient dissociations are exacerbated by the passage of the protein/DNA through the gel; equally however, protein-DNA interactions are enhanced during single molecule experiments due to rapid rebinding (32). Together, this may explain why single molecule approaches are more sensitive to such binding.

The binding of monomeric bZIP domains to DNA has been suggested previously (33,34). Kohler and Schepartz (2001) inferred that AP-1 prefers a pathway in which cJun and cFos bind DNA as monomers and dimerise on DNA. Our data would support such a model for the case of cFos, however for cJun we only observe dimers on DNA, although this does not preclude rapid dimerization on a timescale faster than our observation time.

The motile behaviour of AP-1 complexes on DNA tightropes reveals pausing

True random walks exhibit a linear relationship between time and their mean square displacement (MSD), therefore α in the equation below will be one.

$$MSD = 2Dt^\alpha$$

Where D is the diffusion constant, t is time and α the diffusive exponent. Pausing on DNA upon recognition of specific binding sites is one origin of non-linearity in the MSD vs time relationship (28,35). By quantifying the quality of the linear relationship with MSD (see methods), we were able to

partition tracks into pausing and randomly diffusing populations (Figure 5a). From this analysis, we found 26% of cJun kymographs showed pauses, compared to 44% for cFos and 54% for cJun:cFos (Figure 5A). The selection of pausing versus randomly diffusing kymographs was confirmed by calculating their diffusive exponents, which were significantly lower ($p \leq 0.001$) for paused in all cases (Figure 5B). The observed difference in motility indicates that cJun was more able to randomly diffuse on DNA, while cFos and the heterodimer had a greater number of pauses. This observation suggests that cFos, in a dimer with cJun, imparts a greater pausing propensity to the heterodimeric complex. This is surprising given that they bind identical recognition sequences, therefore the cFos DNA binding domain interacts distinctly from cJun and increases the interaction energy of the whole complex. Further studies to incorporate specific cognate sequences in the absence of even near-cognate sequences (16) are underway to provide more details on the energetics of these interactions.

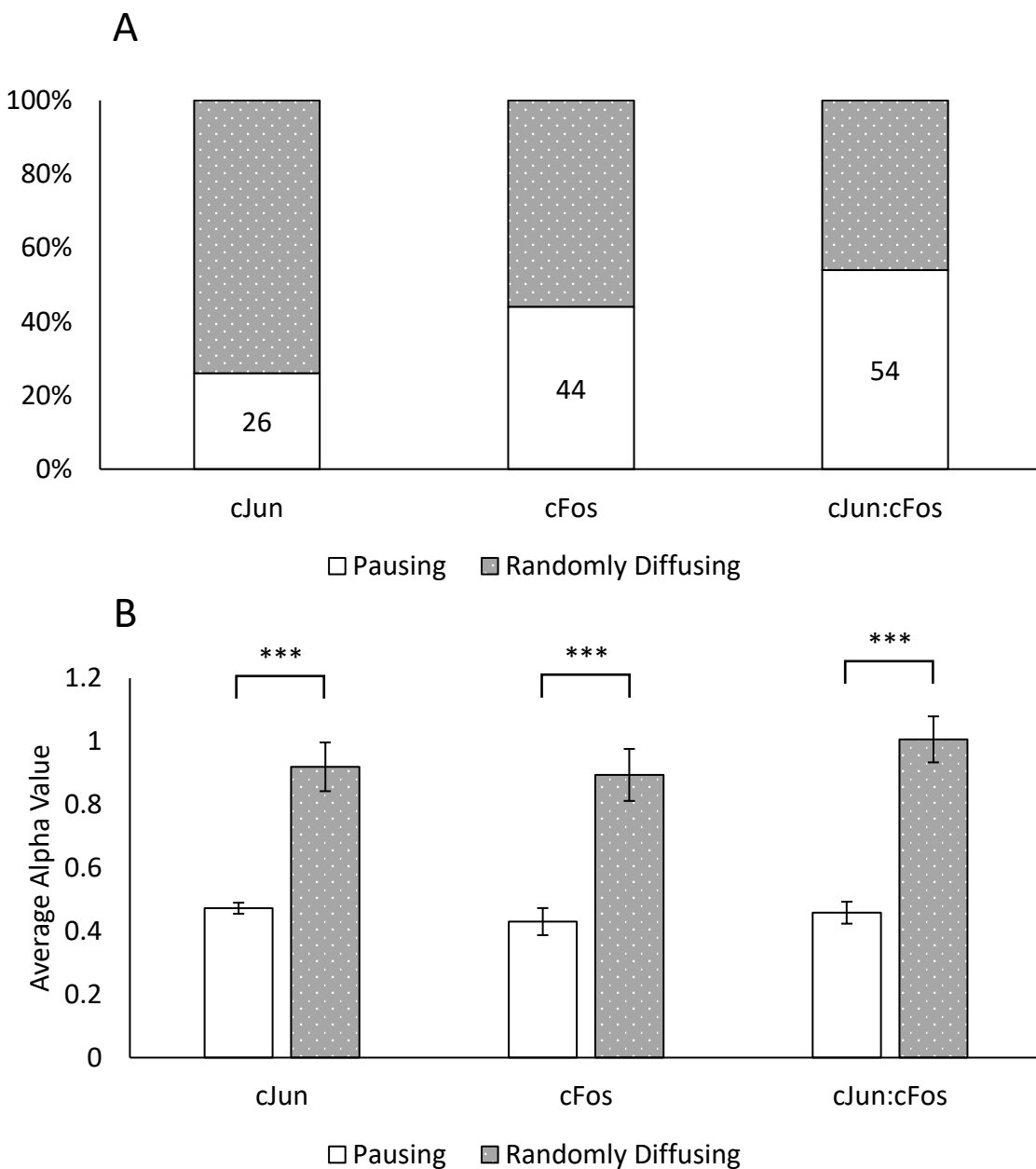


Figure 5: AP-1 proteins show extensive pausing on DNA tightropes. A – Percentages of cJun, cFos and cJun:cFos proteins undergoing pausing. B – Average alpha (α) values for cJun, cFos and cJun:cFos, split between pausing and randomly diffusing kymographs. All three proteins show statistically significant differences between α values for pausing and randomly diffusing ($P \leq 0.001$), $n = 50$ for all proteins; error bars represent SEM of 50 proteins from 5, 10 and 13 flow cells respectively.

The transient nature of transcription factor association (36) could mean these proteins have evolved for temporary interactions that, like other DNA complexes (37), require further partners to enhance binding. In such a way, proteins can initiate a response only when necessary, reducing promoter misfiring. The role of cFos in binding a target site appears to be important within a heterodimer with cJun, however, cFos binding to DNA alone also shows substantial pausing suggesting that the target half-site is enough to trap cFos. Why would monomeric cFos associate with DNA? Would this activate or repress transcription? Perhaps its inability to form homodimers and its propensity to bind half-sites keeps it in the proximity of a promoter such that it is ready to bind an alternative AP-1 partner. Given the ability of cJun to form homodimers, this mechanism may allow a rapid partner swap when cFos is brought to the nucleus.

The data presented in this study indicates that the interactions between DNA and the AP-1 proteins are more nuanced and complex than a simple switch. Rather, multiple heterodimeric and homodimeric partners can exist at the same time and their aggregate effects need to be considered, and no doubt controlled. Surprisingly, we also observe significant numbers of cFos monomers bound to DNA. However, their role is uncertain, do they activate transcription or are they in wait for the right partner? This study sheds new light on a protein complex that lies at the heart of transformation. We have a clearer view of the complexity of this system, and with this understanding we can begin to develop and design better inhibitors capable of selectively targeting the desired species.

Data availability

All data will be made available upon request through the University of Kent academic repository (<https://kar.kent.ac.uk/>).

Acknowledgements

We would like to thank the members of the Kad group, past and present, for useful discussions. This work was supported by the Biotechnology and Biological Sciences Research Council BB/R017921/1, BB/P00847X/1 to NMK and BB/R017956/1 to JMM. JMM is grateful to Cancer Research UK (A26941) and to the EPSRC (EP/M001873/2). The authors declare no conflict of interest.

Author contributions

Collected data: JTL, NAD. Designed experiments: JTL, NAD, JMM, NMK. Analysed Data: JTL, NMK. Wrote paper: JTL, JMM, NMK.

References

1. Shaulian, E. and Karin, M. (2001) AP-1 in cell proliferation and survival. *Oncogene*, **20**, 2390-2400.
2. Halazonetis, T.D., Georgopoulos, K., Greenberg, M.E. and Leder, P. (1988) c-Jun dimerizes with itself and with c-Fos, forming complexes of different DNA binding affinities. *Cell*, **55**, 917-924.
3. Glover, J.N. and Harrison, S.C. (1995) Crystal structure of the heterodimeric bZIP transcription factor c-Fos-c-Jun bound to DNA. *Nature*, **373**, 257-261.
4. Jochum, W., Passegue, E. and Wagner, E.F. (2001) AP-1 in mouse development and tumorigenesis. *Oncogene*, **20**, 2401-2412.
5. Eckert, R.L., Adhikary, G., Young, C.A., Jans, R., Crish, J.F., Xu, W. and Rorke, E.A. (2013) AP1 transcription factors in epidermal differentiation and skin cancer. *J Skin Cancer*, **2013**, 537028.
6. Liu, G., Ye, X., Miller, E.J. and Liu, S.F. (2014) NF-kappaB-to-AP-1 switch: a mechanism regulating transition from endothelial barrier injury to repair in endotoxemic mice. *Scientific reports*, **4**, 5543.
7. Webster, K.A., Discher, D.J. and Bishopric, N.H. (1994) Regulation of fos and jun immediate-early genes by redox or metabolic stress in cardiac myocytes. *Circ Res*, **74**, 679-686.
8. Bahrami, S. and Drablos, F. (2016) Gene regulation in the immediate-early response process. *Adv Biol Regul*, **62**, 37-49.
9. Lv, X., Wang, H., Su, A., Xu, S. and Chu, Y. (2018) Herpes simplex virus type 2 infection triggers AP-1 transcription activity through TLR4 signaling in genital epithelial cells. *Virol J*, **15**, 173.
10. Eferl, R. and Wagner, E.F. (2003) AP-1: a double-edged sword in tumorigenesis. *Nat Rev Cancer*, **3**, 859-868.
11. Shen, Q., Uray, I.P., Li, Y., Krisko, T.I., Strecker, T.E., Kim, H.T. and Brown, P.H. (2008) The AP-1 transcription factor regulates breast cancer cell growth via cyclins and E2F factors. *Oncogene*, **27**, 366-377.
12. Ashida, R., Tominaga, K., Sasaki, E., Watanabe, T., Fujiwara, Y., Oshitani, N., Higuchi, K., Mitsuyama, S., Iwao, H. and Arakawa, T. (2005) AP-1 and colorectal cancer. *Inflammopharmacology*, **13**, 113-125.

13. Vleugel, M.M., Greijer, A.E., Bos, R., van der Wall, E. and van Diest, P.J. (2006) c-Jun activation is associated with proliferation and angiogenesis in invasive breast cancer. *Hum Pathol*, **37**, 668-674.
14. Mason, J.M., Schmitz, M.A., Muller, K.M. and Arndt, K.M. (2006) Semirational design of Jun-Fos coiled coils with increased affinity: Universal implications for leucine zipper prediction and design. *Proc Natl Acad Sci U S A*, **103**, 8989-8994.
15. Leaner, V.D., Donninger, H. and Birrer, M.J. (2007) Transcription factors as targets for cancer therapy: AP-1 a potential therapeutic target. *Current Cancer Therapy Reviews*, **3**, 1-6.
16. Seldeen, K.L., McDonald, C.B., Deegan, B.J. and Farooq, A. (2009) Single nucleotide variants of the TGACTCA motif modulate energetics and orientation of binding of the Jun-Fos heterodimeric transcription factor. *Biochemistry*, **48**, 1975-1983.
17. Hai, T. and Curran, T. (1991) Cross-family dimerization of transcription factors Fos/Jun and ATF/CREB alters DNA binding specificity. *Proc Natl Acad Sci U S A*, **88**, 3720-3724.
18. Seldeen, K.L., McDonald, C.B., Deegan, B.J., Bhat, V. and Farooq, A. (2009) DNA plasticity is a key determinant of the energetics of binding of Jun-Fos heterodimeric transcription factor to genetic variants of TGACGTCA motif. *Biochemistry*, **48**, 12213-12222.
19. Zhou, H., Zarubin, T., Ji, Z., Min, Z., Zhu, W., Downey, J.S., Lin, S. and Han, J. (2005) Frequency and distribution of AP-1 sites in the human genome. *DNA Res*, **12**, 139-150.
20. Nakabeppu, Y., Ryder, K. and Nathans, D. (1988) DNA binding activities of three murine Jun proteins: stimulation by Fos. *Cell*, **55**, 907-915.
21. Grondin, B., Lefrancois, M., Tremblay, M., Saint-Denis, M., Haman, A., Waga, K., Bedard, A., Tenen, D.G. and Hoang, T. (2007) c-Jun homodimers can function as a context-specific coactivator. *Mol Cell Biol*, **27**, 2919-2933.
22. O'Shea, E.K., Rutkowski, R., Stafford, W.F., 3rd and Kim, P.S. (1989) Preferential heterodimer formation by isolated leucine zippers from fos and jun. *Science*, **245**, 646-648.
23. Smeal, T., Angel, P., Meek, J. and Karin, M. (1989) Different requirements for formation of Jun: Jun and Jun: Fos complexes. *Genes Dev*, **3**, 2091-2100.
24. Szaloki, N., Krieger, J.W., Komaromi, I., Toth, K. and Vamosi, G. (2015) Evidence for Homodimerization of the c-Fos Transcription Factor in Live Cells Revealed by Fluorescence Microscopy and Computer Modeling. *Mol Cell Biol*, **35**, 3785-3798.
25. Kad, N.M., Wang, H., Kennedy, G.G., Warshaw, D.M. and Van Houten, B. (2010) Collaborative dynamic DNA scanning by nucleotide excision repair proteins investigated by single- molecule imaging of quantum-dot-labeled proteins. *Mol Cell*, **37**, 702-713.
26. Springall, L., Inchingolo, A.V. and Kad, N.M. (2016) DNA-Protein Interactions Studied Directly Using Single Molecule Fluorescence Imaging of Quantum Dot Tagged Proteins Moving on DNA Tightropes. *Chromosome Architecture: Methods and Protocols*, 141-150.
27. Hughes, C.D., Wang, H., Ghodke, H., Simons, M., Towheed, A., Peng, Y., Van Houten, B. and Kad, N.M. (2013) Real-time single-molecule imaging reveals a direct interaction between UvrC and UvrB on DNA tightropes. *Nucleic Acids Res*, **41**, 4901-4912.
28. Barbi, M., Place, C., Popkov, V. and Salerno, M. (2004) A model of sequence-dependent protein diffusion along DNA. *J Biol Phys*, **30**, 203-226.
29. Hess, J., Angel, P. and Schorpp-Kistner, M. (2004) AP-1 subunits: quarrel and harmony among siblings. *J. Cell Sci.*, **117**, 5965-5973.
30. Schurr, J.M. (1979) The one-dimensional diffusion coefficient of proteins absorbed on DNA. Hydrodynamic considerations. *Biophys Chem*, **9**, 413-414.
31. Kuno, M., Fromm, D.P., Hamann, H.F., Gallagher, A. and Nesbitt, D.J. (2000) Nonexponential "blinking" kinetics of single CdSe quantum dots: A universal power law behavior. *Journal of Chemical Physics*, **112**, 3117-3120.
32. Graham, J.S., Johnson, R.C. and Marko, J.F. (2011) Concentration-dependent exchange accelerates turnover of proteins bound to double-stranded DNA. *Nucleic Acids Res*, **39**, 2249-2259.

33. Cranz, S., Berger, C., Baici, A., Jelesarov, I. and Bosshard, H.R. (2004) Monomeric and dimeric bZIP transcription factor GCN4 bind at the same rate to their target DNA site. *Biochemistry*, **43**, 718-727.
34. Kohler, J.J. and Schepartz, A. (2001) Kinetic studies of Fos.Jun.DNA complex formation: DNA binding prior to dimerization. *Biochemistry*, **40**, 130-142.
35. Dunn, A.R., Kad, N.M., Nelson, S.R., Warshaw, D.M. and Wallace, S.S. (2011) Single Qdot-labeled glycosylase molecules use a wedge amino acid to probe for lesions while scanning along DNA. *Nucleic Acids Res*, **39**, 7487-7498.
36. Elf, J., Li, G.W. and Xie, X.S. (2007) Probing transcription factor dynamics at the single-molecule level in a living cell. *Science*, **316**, 1191-1194.
37. Lin, J., Countryman, P., Buncher, N., Kaur, P., E, L., Zhang, Y., Gibson, G., You, C., Watkins, S.C., Piehler, J. *et al.* (2014) TRF1 and TRF2 use different mechanisms to find telomeric DNA but share a novel mechanism to search for protein partners at telomeres. *Nucleic Acids Res*, **42**, 2493-2504.
38. Slutsky, M. and Mirny, L.A. (2004) Kinetics of protein-DNA interaction: facilitated target location in sequence-dependent potential. *Biophys J*, **87**, 4021-4035.

Supplementary Information

Correcting diffusion constants for the presence of Qdots

To calculate the frictional energy barrier to free motion on DNA we calculated the stepping rate from the measured diffusion constant (D) per second assuming single base pair steps (l) for a Qdot labelled complex that rotationally follows the DNA helix (30):

$$Steps/s = 2D/l^2$$

Based upon the hydrodynamic radius of the protein-Qdot complex (~ 13 nm) we estimate the barrier-less diffusion constant to calculate the expected maximum stepping rate (27). The relative stepping rate provides the energy barrier when the Arrhenius relationship is applied:

$$Steps/s = e^{-(E_{A1}-E_{A2})/kT},$$

$$\therefore \text{energy barrier (in } kT) = \ln \left(\frac{Steps_{max}}{s} / \frac{Steps_{meas}}{s} \right) = \ln (D_{max}/D_{meas})$$

Where $Steps_{meas}$ can be derived from the measured diffusion constant and $Steps_{max}$ is the maximum theoretical stepping rate. k is the Boltzmann constant and T is temperature in Kelvin. Removing the contribution of the Qdot from the hydrodynamic radius allows us to derive the expected maximum stepping rate of the protein alone. Using the energy barrier value calculated here permits back-calculation of the protein's diffusion constant without a Qdot.

The values for the energy barriers given in the main text are very low and within the optimum searching parameters suggested by previous modeling studies (38). Such low values indicate a very rapid search of the DNA and support the assumption that the proteins follow the DNA groove. Diffusion without following the groove would be much faster, and to achieve the observed diffusion constants would require very high energy barriers to diffusion of ~ 9 kT.